scientific reports

Check for updates

OPEN

Denervation of rectus capitis posterior minor as neglected factor in Chiari malformation type I revealed by double blinded prospective study

Yunsen He[1], Qinjiang Huang[3], Mingbin Bao[2], Mengjun Zhang[4], Xiaolin Hou[2], Ping Liu[2], Ye Tao[2], Hongliang Li[1], Kun Li[1], Li Liu[6], Lili Guo[2], Hao Wang[7], Zhou Zhang[5]✉ & Bo Wu[2]✉

Chiari malformation type I (CMI) typically manifests with Valsalva-induced occipital headaches and commonly co-occurs with syringomyelia. The disruption of cerebrospinal fluid (CSF) dynamics at the craniocervical junction (CCJ) is a key pathophysiological feature. The rectus capitis posterior minor (RCPmi), innervated by the C1 nerve root's posterior branch, significantly facilitates CSF flow at the CCJ, correlating closely with occipital headaches. This study aims to explore RCPmi functionality in CMI patients compared to healthy controls using needle electromyography (nEMG). Data from adult CMI patients and a health group collected from January 2023 to May 2024 were analyzed. Both groups underwent bilateral RCPmi nEMG testing, assessing mean duration, amplitude, multiphasic wave ratio, recruitment phase amplitude, and spontaneous potentials during Valsalva maneuvers. We conducted a double-blinded evaluation, with additional subgroup analyses based on headache presence, tonsillar herniation relative to the C1 vertebra, and syringomyelia involvement. The study included 40 CMI patients and 30 healthy controls with no demographic differences. Healthy controls displayed stable RCPmi-nEMG parameters, with intense electrical activity during Valsalva maneuvers. In contrast, CMI patients exhibited substantial denervation damage in bilateral RCPmi, particularly during Valsalva maneuvers, characterized by insufficient electrical signal response and sparse motor units. Subgroup analysis revealed increased denervation in patients with headaches, extensive tonsillar herniation, and syringomyelia involving C1. RCPmi plays a critical role in maintaining cranio-cervical stability and modulating intracranial pressure, especially during Valsalva maneuvers. Compared to controls, CMI patients show widespread denervation damage in RCPmi, strongly linked to enhanced obstruction of CCJ-CSF flow and typical headache symptoms. This denervation damage, likely related to pathological factors like C1 nerve root compression by herniated cerebellar tonsils and inflammatory mediator release at the CCJ, highlights the functional failure of RCPmi as a novel target for understanding the headache mechanism in CMI and for developing pain interventions.

Keywords Chiari malformarion type I, Rectus capitis posterior minor, Needle electromyographical, Headache, C1 nerve root, Syringomyelia, Cerebellar tonsil, Myodural bridge

[1]Department of Neurosurgery, Sichuan Lansheng Brain Hospital and Shanghai Lansheng Brain Hospital Investment Co., Ltd., Chengdu 610036, Sichuan, People's Republic of China. [2]Department of Neurosurgery, Sichuan Provincial People's Hospital, University of Electronic Science and Technology of China, No.32, West Section 2, First Ring Road, Chengdu 610072, Sichuan, People's Republic of China. [3]Department of Neurosurgery, Chengdu wenjiang District people's hospital, Chengdu 611130, Sichuan, People's Republic of China. [4]Department of Neuropsychology, Sichuan Provincial Center for Mental Health, Sichuan Provincial People's Hospital, University of Electronic Science and Technology of China, Chengdu 610072, Sichuan, People's Republic of China. [5]Department of Rehabilitation, Sichuan Provincial People's Hospital, University of Electronic Science and Technology of China, No.32, West Section 2, First Ring Road, Chengdu 610072, Sichuan, People's Republic of China. [6]Department of Radiology, Sichuan Provincial People's Hospital, University of Electronic Science and Technology of China, Chengdu 610072, Sichuan, People's Republic of China. [7]Department of Neurosurgery, Jianyang Chinese Medicine Hospital, Chengdu 641400, Sichuan, People's Republic of China. ✉email: z.gabriel@163.com; wuboscph@sina.com

Basic introduction to CMI

Chiari malformation (CM), first described by Austrian pathologist Hans Chiari in 1891[1], is divided into four types, with type I (CMI) being the most prevalent clinically. The characteristic symptom of CMI is occipitocervical Valsalva-induced headaches (45%), but some patients (29%) exhibit atypical headache symptoms, mainly migraines[2]. Due to its frequent comorbidity with syringomyelia, it significantly impacts the life quality of affected individuals. Posterior fossa decompression (PFD) is the current mainstream treatment, though the specific surgical approach remains controversial[3,4].

Etiological controversy and the function of RCPmi in CMI

CMI has traditionally been attributed to mesodermal underdevelopment leading to congenital insufficiency of posterior fossa (PCF) volume, causing normal cerebellar and cerebellar tonsil development to be displaced into the cervical area, obstructing cerebrospinal fluid (CSF) flow at the craniocervical junction (CCJ)[1–5]. However, some CMI patients do not exhibit narrowed PCF[6], and numerous cases of acquired CMI have been increasingly reported[1,7,8]. Thus, the congenital pathogenesis theory of CMI is widely challenged, prompting the proposal of numerous new etiological theories[1].

It is widely believed that obstruction of the CCJ-CSF pathway by herniated cerebellar tonsils, leading to disturbances in CCJ-CSF hydrodynamics, is a primary pathogenic factor[4]. Recent studies have shown that during contraction, RCPmi can modulate the tension of the dural membranes at the CCJ through myodural bridges (MDBs), thereby facilitating CSF flow[9,10]. Thus, RCPmi plays a crucial role in the pathophysiological mechanism of CMI.

Moreover, research on cervical-occipital instability in CMI patients continues to emerge, strongly linking with the function of RCPmi in balancing the atlanto-occipital joint[9,10]. Early on, Goel posited that all CMI patients exhibit atlantoaxial instability, suggesting it as the true cause of CMI, a viewpoint that remains controversial[11,12]. Subsequently, Wan and colleagues observed that the atlanto-occipital joints in CMI patients are extremely flat and asymmetrical, suggesting that these morphological variations might contribute to instability and possibly to the etiology of CMI[13,14]. Later, Ravindra and colleagues introduced a new radiographic indicator, the C–C2 Sagittal Vertical Axis (C2SVA), to quantify cervical-occipital instability in CMI patients, suggesting that a C2SVA ≥ 5 mm indicates instability[13,14]. Recently, Labuda and colleagues hypothesized that "subclinical instability" at the CCJ causes continuous strain on muscles like RCPmi, leading to MDBs overload and subsequently to disturbances in CCJ-CSF circulation[15].

RCPmi is critically involved in both CCJ-CSF circulation and cervical-occipital stability, making the study of its functional status essential.

Study objectives

Although there have been reports on the surface electromyography (sEMG) of RCPmi in normal populations[16–18], there are currently no studies on the needle electromyography (nEMG) of RCPmi in CMI patients. Therefore, the objectives of this study are to explore: (1) the nEMG parameters of RCPmi in a healthy adult population; (2) the nEMG characteristics and presence of denervation damage in RCPmi of CMI patients; (3) the pathophysiological mechanisms causing denervation damage in RCPmi of CMI patients; (4) new pathophysiological mechanisms and interventional targets based on RCPmi denervation damage in CMI.

Methods

Ethical approval and informed consent

We selected CMI patients treated at the Neurosurgery Department of Sichuan Provincial People's Hospital between January 2023 and May 2024. A control group of healthy individuals with no demographic differences was also recruited.

Initially, the feasibility and safety of the study were thoroughly discussed within our research team based on previous reports' protocols[16–19]. The study was then registered with and approved by the Ethics Committee of Sichuan Provincial People's Hospital (available at https://www.samsph.com/), which included an ethical review. All participants were informed of the potential risks associated with nEMG and signed an informed consent form. Our research team will protect the privacy and personal information security of the participants, ensure the confidentiality of the data, and use it solely for the purpose of this study. This study strictly adheres to applicable national and international regulations and ethical standards, including but not limited to the Declaration of Helsinki. Any unexpected harm that occurs during the research process will be properly handled by the research team and reported to the ethics committee. The datasets used and/or analyzed during the current study available from the corresponding author on reasonable request.

Participant inclusion and exclusion criteria

Inclusion criteria: Patients with "sample CMI"[1] treated at our facility (excluding those with atlanto-occipital fusion, basilar invagination, atlantoaxial dislocation, hydrocephalus, scoliosis, etc.).

Exclusion criteria: (1) Incomplete research data; (2) History of cranio-cervical trauma (especially Whiplash injuries) or high cervical disc herniation that could damage the C1 nerve or RCPmi; (3) Age < 18 or > 80 years; (4) Contraindications to nEMG of RCPmi (including those with CVJ occupying lesions, infections, vascular malformations; coagulation disorders; dermatitis in the posterior cervical region).

Double-blinded testing

CMI patients and healthy controls were independently recruited by our Center of Neurology (combining departments of Neurosurgery and Neurology). The nEMG testing and assessment were independently performed by our Electrophysiology Center, maintaining blinding of both the testers and the subjects.

nEMG testing methods for RCPmi

Puncture method

Prior to puncture, head and neck magnetic resonance images (MRI)was used to exclude vascular malformations and other contraindications at the CCJ in patients. RCPmi's superficial position and depth were further measured on 3D-T1 equence according to the method described by Richard's team[16]. The exact puncture sites on the body surface were located using three-dimensional reconstruction shadow techniques (Fig. 1A–E) and marked on the patient's CCJ (Fig. 1F). The room temperature was maintained between 25 °C and 32 °C during tests. After

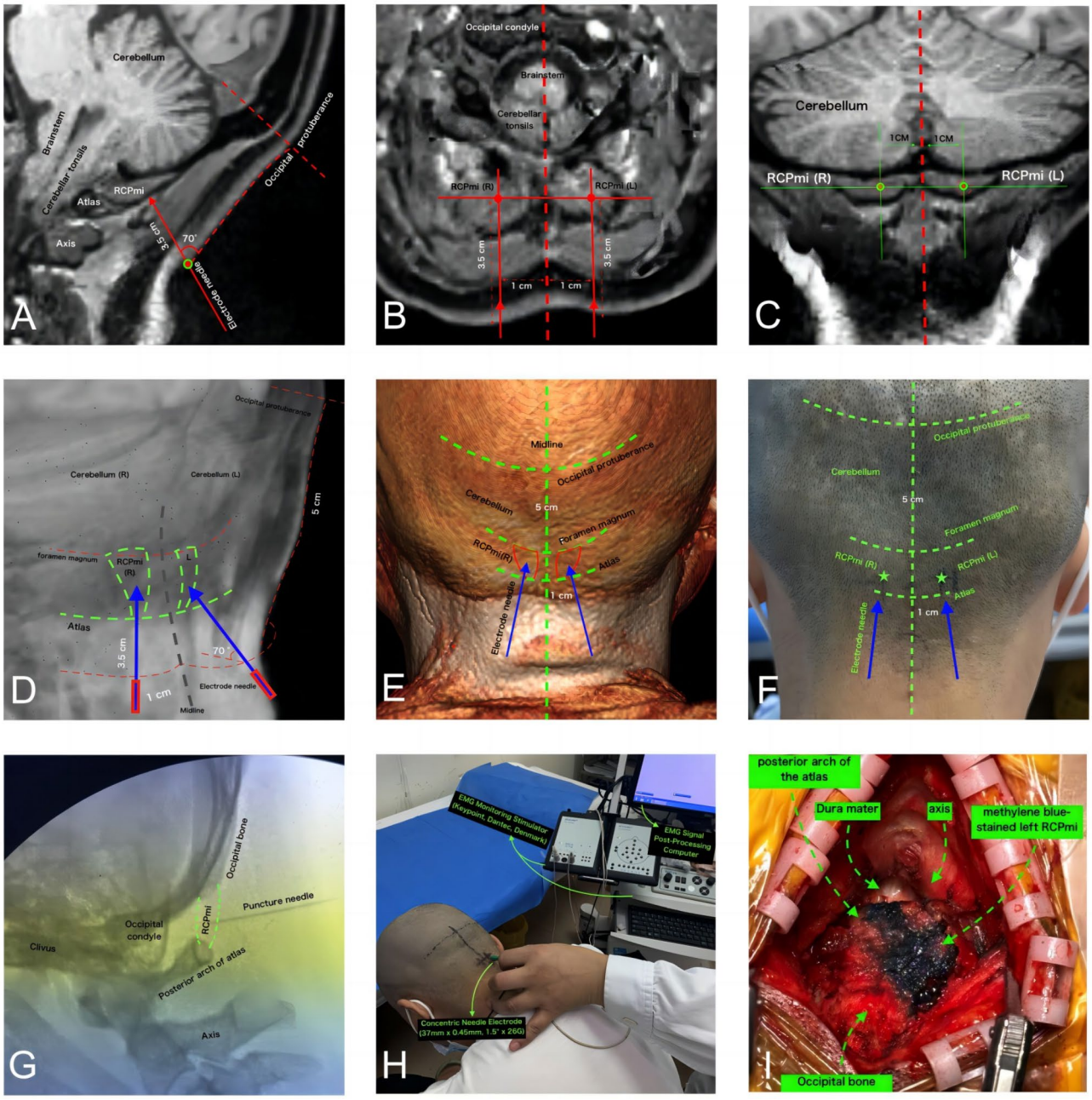

Fig. 1. Reference diagram for nEMG puncture localization of RCPmi. (**A**) Pre-puncture, head and neck 3D-T1 sequence, sagittal view near midline RCPmi localization slice. (**B**) Pre-puncture, head and neck 3D-T1 sequence, axial view RCPmi localization slice. (**C**) Pre-puncture, head and neck 3D-T1 sequence, coronal view RCPmi localization slice. (**D**) Pre-puncture, head and neck 3D-T1 sequence, 3D perspective reconstruction localization slice. (**E**) Pre-puncture, head and neck 3D-T1 sequence, 3D body surface reconstruction localization slice. (**F**) Localization diagram of RCPmi puncture site on the subject. (**G**) Intraoperative C-arm X-ray sagittal localization diagram during puncture. (**H**) Patient condition during nEMG testing. (**I**) Preoperative nEMG examination puncture using methylene blue to stain RCPmi, immediately followed by posterior cranial fossa decompression surgery to verify puncture accuracy. Results show that the deep blue part is the left side RCPmi, accurately punctured. *RCPmi* rectus capitis posterior minor, *EMG* electromyogram.

strict disinfection, puncture was performed under nerve navigation (Fig. 1G), and once the correct position was confirmed, data monitoring commenced (Fig. 1H).

Verification of puncture accuracy
Ten CMI patients scheduled for posterior decompression surgery were randomly selected for puncture using the concentric circle needle technique (single-use lumbar puncture needle—Medtronic). After positioning, 0.5 ml of sterile methylene blue was injected within the hollow needle. Verification was conducted during the posterior decompression surgery, confirming accurate placement within the RCPmi (Fig. 1I). The accuracy rate was 100%.

Signal processing
Concentric circle needle electrodes (37 mm × 0.45 mm, 1.5″ × 26G) were inserted and connected to a neurological electrophysiological monitoring stimulator (Keypoint-four channels-Dantec, Denmark) (Fig. 1H). Signals with missing baseline or excessive noise were corrected. Original nEMG voltages were amplified, passed through a band-pass filter (20–10,000 Hz), and digitized at 3000 samples per second. Data corrections were performed using software developed in Matlab (The Mathworks), which involved removing offset voltages and QRS waves, with a low-pass filter cutoff at 0.5 Hz. nEMG data were collected consistently to ascertain baseline activity/noise values, ensuring that each data channel was free of noise and artifacts.

Data collection
nEMG assessments of the left and right Rectus Capitis Posterior Minor were performed sequentially. Measurements included spontaneous potentials at rest, average latency, and average amplitude of motor unit action potentials (MUAPs) during light contraction, the proportion of multiphasic waves (%), amplitude, and recruitment phases during intense contraction (IP), as well as nEMG images during coughing (with the head and neck stationary). At rest, the presence of two or more fibrillation potentials or sharp waves in the same muscle was considered abnormal. During intense contraction, recruitment phase potentials were classified as normal if presenting as simple or simple-mixed phases; a purely simple phase during intense contraction suggested abnormalities, whereas mixed and interference phases were deemed normal.

Follow-up
After monitoring was completed, the puncture needle was removed, the puncture site was disinfected again, and a bandage was applied. Cardiac monitoring was conducted for 30 min. Participants then entered a follow-up phase, during which a unified head and neck MRI assessment was performed at one year as precious research[19].

Statistical analysis
Data analyses were conducted using SPSS 25.0 and Graphpad Prism 9.5. Quantitative data following a normal distribution were expressed as mean ± standard deviation ($\bar{X} \pm \sigma$) and comparisons between groups were made using t-tests. For non-normally distributed quantitative data, medians (interquartile ranges) M (IQR) were used, and group comparisons were performed using the Mann-Whitney U test. Categorical data were presented as frequencies (n) and percentages (%), with comparisons made using the Chi-square test. All analyses were two-tailed, with a p value < 0.05 considered statistically significant.

Data availability
The datasets used and/or analysed during the current study available from the corresponding author on reasonable request.

Result
Demographic information
We prospectively collected data from 40 CMI patients (22 females, 18 males; average age = 45.88 years) and 30 healthy controls (21 females, 9 males; average age = 49.10 years), with no demographic differences between the groups (Table 1). In the CMI group, the average tonsillar herniation (TH) was 8.76 mm, with 25 cases (62.5%) experiencing headaches, and 27 cases (67.5%) having syringomyelia adjacent to the C1 segment.

nEMG data for healthy controls
In healthy adults, RCPmi during mild contraction showed average latencies of 10.40 ms (R/L) and average amplitudes of 353.00/364.50 μV, with a very low proportion of multiphasic waves. After removing multiphasic wave interference, the adjusted average latencies were 10.35/10.50 ms (R/L) (Fig. 2A). During intense contractions, interference pattern amplitudes were 1.65/1.56 mV (R/L), with recruitment phases predominantly showing interference patterns (Fig. 2B); at rest, RCPmi exhibited essentially no spontaneous abnormal potentials

	Health (N1 = 30)	CMI (N2 = 40)	X2/Z	*p* value
Sex			1.628	0.202
F	21 (70.00%)	22 (55.00%)		
M	9 (30.00%)	18 (45.00%)		
Age	49.10 ± 12.466	45.88 ± 10.608	1.167	0.247

Table 1. Demographic basic information of the included healthy population and CMI patients.

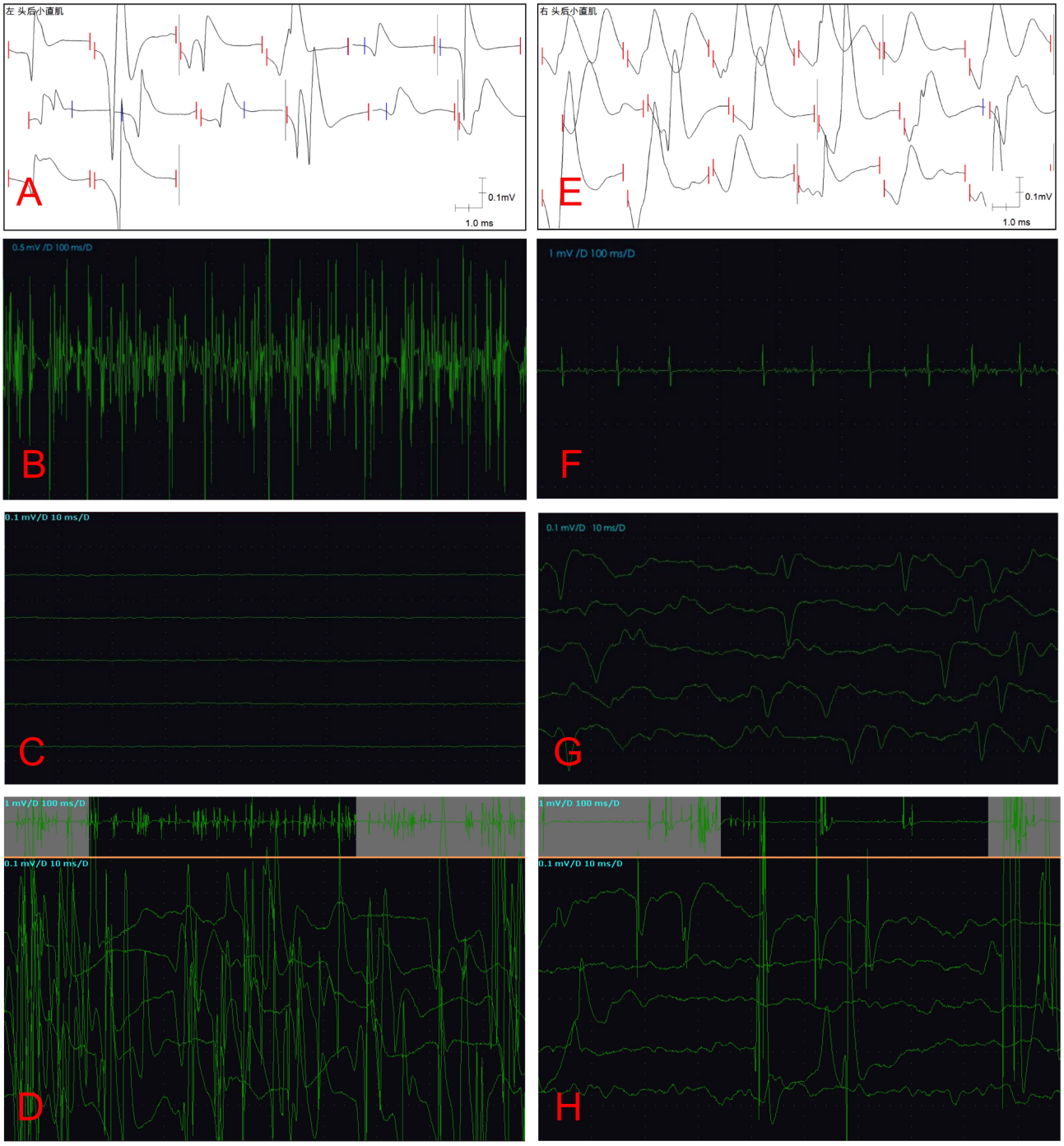

Fig. 2. Typical nEMG graphs of healthy adults and CMI patients. (**A**–**D**) Typical feature graphs of RCPmi nEMG in healthy adults. Figure (**A**) Motor unit action potential (MUAP) graph during light contraction, showing that motor units have relatively short average durations, not high average amplitudes, and very low multiphasic wave ratios. Figure (**B**) High interference amplitude during intense contraction, with recruitment phases as interference phases. Figure (**C**) RCPmi shows no spontaneous abnormal potentials at rest. Figure (**D**) During coughing or other Valsalva maneuvers, RCPmi has instantaneous ultra-high amplitudes, with many motor units instantly activated. (**E**–**H**) Typical feature graphs of RCPmi nEMG in CMI patients. Figure (**E**) Motor unit action potential (MUAP) graph during light contraction, showing that motor units have relatively long average durations, relatively high average amplitudes, and high multiphasic wave ratios. Figure (**F**) Low interference amplitude during intense contraction, with recruitment phases as simple phases. Figure (**G**) RCPmi often shows spontaneous abnormal potentials at rest. Figure (**H**) During coughing or other Valsalva maneuvers, RCPmi shows delayed, desynchronized low amplitude discharges, with fewer motor units activated.

(Fig. 2C). During coughing or other Valsalva maneuvers, RCPmi exhibited intensely high contraction amplitudes (Fig. 2D). RCPmi-EMG parameters in healthy adults showed no significant relationship with sex or age (18–69 years). Detailed nEMG data for the control group are provided in Table 2.

nEMG data for CMI patients

Compared to the healthy control group, CMI patients exhibited significantly prolonged average latencies (R/L = 11.70/11.85 ms) and increased average amplitudes ($P > 0.05$). The proportion of multiphasic waves was significantly higher, and the Polyphasic-Adjusted Average Latency was also significantly prolonged (R/L = 11.44/11.70 ms) (Fig. 2E). During intense contractions, interference amplitude was reduced (not statistically significant, $P > 0.05$), and recruitment phases mainly showed simple phases (Fig. 2F). At rest, the proportion of spontaneous abnormal potentials was significantly higher (Fig. 2G). During coughing or other Valsalva maneuvers, RCPmi demonstrated delayed, desynchronized, sparse wave discharges with fewer motor units activated (Fig. 2H). Typical nEMG differences are shown in Fig. 2, with specific data and differences detailed in Table 2; Fig. 3.

CMI headache group versus non-headache group nEMG differences

There were no demographic differences between the headache and non-headache groups within the CMI patients. Compared to the non-headache group, the headache group showed further prolongation in Average Latency and Polyphasic-Adjusted Average Latency, and an increase in Average Amplitude ($P > 0.05$). Other parameters showed no significant differences. Specific data and differences are detailed in Table 3; Fig. 3.

nEMG differences between CMI patients with tonsillar herniation exceeding C1 and those not exceeding C1

Compared to the group where tonsillar herniation (TH) did not exceed C1, the group with TH exceeding C1 showed further prolongation in average latency and polyphasic-adjusted average latency; average amplitude was also higher ($P > 0.05$). Other parameters showed no significant differences. Specific data and differences are detailed in Table 4; Fig. 3.

Parameters	Health (N1 = 30)	CMI (N2 = 40)	X^2/ Z/t	*p* value
Average latency (ms) (R)	**10.40 (9.48, 10.90)**	**11.70 (10.20, 12.80)**	**−3.788**	**0.000**
Average latency (ms) (L)	**10.40 (9.15, 10.90)**	**11.85 (10.58, 13.18)**	**−4.257**	**0.000**
Average amplitude (Uv) (R)	353.00 (291.00, 382.50)	375.00 (321.00, 436.75)	−1.507	0.132
Average amplitude (uv) (L)	364.50 (284.00, 395.75)	370.00 (302.50, 458.00)	−0.76	0.447
Polyphasic wave ratio % (R)	**0.00 (0.00, 10.05)**	**8.35 (0.00, 12.93)**	**−2.092**	**0.036**
Polyphasic wave ratio % (L)	7.10 (0.00, 10.65)	6.10 (0.00, 12.33)	−0.505	0.614
Polyphasic-adjusted average latency (R)	**10.35 ± 1.19**	**11.44 ± 1.59**	**−3.175**	**0.002**
Polyphasic-adjusted average latency (L)	**10.50 (9.50, 10.90)**	**11.7 (10.50, 12.98)**	**−3.848**	**0.000**
Amplitude mv (R)	1.65 (1.30, 1.80)	1.50 (1.20, 1.80)	−0.841	0.401
Amplitude mv (L)	1.56 ± 0.35	1.45 ± 0.43	1.163	0.249
Recruitment phase (R)			**17.078**	**0.000**
0	26 (86.70)	15 (37.50)		
1	4 (13.30)	25 (62.50)		
Recruitment phase (L)			**28.078**	**0.000**
0	28 (93.30)	12 (30.00)		
1	2 (6.70)	28 (70.00)		
Spontaneous abnormal potentials (R)			**10**	**0.002**
0	27 (90.00)	22 (55.00)		
1	3 (10.00)	18 (45.00)		
Spontaneous abnormal potentials (L)			**10**	**0.002**
0	27 (90.00)	22 (55.00)		
1	3 (10.00)	18 (45.00)		

Table 2. Comparison of electrophysiological parameters between healthy individuals and CMI patients. R represents the right RCPmi, and L represents the left RCPmi. Parameters with statistical differences are highlighted in bold. In the recruitment phase, "0" represents interference or mixed pattern, while "1" represents simple pattern. In spontaneous abnormal potentials, "0" represents the absence of any noticeable spontaneous abnormal potentials, while "1" indicates the presence of various patterns of spontaneous abnormal potentials detected.

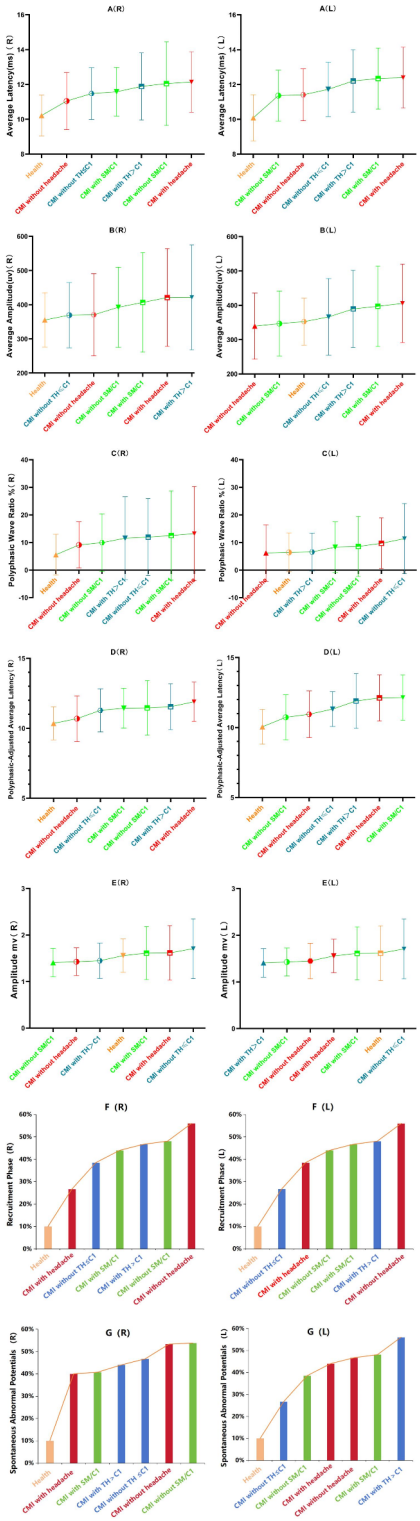

Fig. 3. Display of differences in nEMG parameters between healthy adults and CMI patient subgroups. The vertical axis represents parameter names, and the horizontal axis represents groups. Figures (**A (R)**)–(**G (R)**) represent the nEMG parameters of the right RCPmi. Figures (**A (L)**)–(**G (L)**) represent the nEMG parameters of the left RCPmi. Brown represents the healthy group. CMI patient subgroups are marked with common colors: red represents the CMI headache and non-headache groups, blue represents the cerebellar tonsil herniation (TH) groups exceeding or not exceeding C1, and green represents the syringomyelia (SM) groups involving or not involving C1. Figures (**A**–**E**) data are continuous numerical parameters, represented by error bar plots, while (**F**–**G**) are proportional values (%), represented by bar graphs. C1 the first cervical vertebra, *TH* tonsillar herniation, *SM/C1* syringomyelia involving the C1 vertebra.

Variable	Headache No (N1 = 15)	Headache Yes (N2 = 25)	X^2/ Z/t	*p* value
Sex			0.242	0.622
Female	9 (60.00)	13 (52.00)		
Male	6 (40.00)	12 (48.00)		
Age (median, interquartile range)	48.00 (38.00, 53.00)	49.00 (38.00, 55.50)	−0.573	0.566
Average latency (ms) (R)	**11.10 (9.70, 12.80)**	**11.90 (11.15, 12.95)**	**−1.985**	**0.047**
Average latency (ms) (L)	11.70 (9.80, 13.10)	12.10 (11.00, 13.60)	−1.593	0.111
Average amplitude (uv) (R)	364.00 (291.00, 410.00)	377.00 (350.00, 469.50)	−1.215	0.224
Average amplitude (uv) (L)	339.33 ± 96.52	405.44 ± 114.3	−1.873	0.069
Polyphasic wave ratio % (R)	9.10 (0.00, 13.30)	7.70 (2.40, 12.70)	−0.014	0.989
Polyphasic wave ratio % (L)	0.00 (0.00, 7.50)	8.70 (0.00, 16.30)	−1.766	0.077
Polyphasic-adjusted average latency (R)	**10.69 ± 1.63**	**11.9 ± 1.40**	**−2.485**	**0.017**
Polyphasic-adjusted average latency (L)	**10.95 ± 1.67**	**12.12 ± 1.64**	**−2.176**	**0.036**
Amplitude mv (R)	1.50 (1.20, 1.60)	1.50 (1.20, 1.95)	−0.941	0.347
Amplitude mv (L)	1.45 ± 0.47	1.45 ± 0.42	−0.009	0.993
Recruitment phase (R)			3.136	0.077
0	3 (20.00)	12 (48.00)		
1	12 (80.00)	13 (52.00)		
Recruitment phase (L)			1.143	0.285
0	3 (20.00)	9 (36.00)		
1	12 (80.00)	16 (64.00)		
Spontaneous abnormal potentials (R)			0.673	0.412
0	7 (46.7)	15 (60)		
1	8 (53.3)	10 (40)		
Spontaneous abnormal potentials (L)			0.027	0.87
0	8 (53.3)	14 (56)		
1	7 (46.7)	11 (44)		

Table 3. Comparison of EMG parameters between CMI patients with and without headaches. R represents the right RCPmi, and L represents the left RCPmi. Parameters with statistical differences are highlighted in bold. In the recruitment phase, "0" represents interference or mixed pattern, while "1" represents simple pattern. In spontaneous abnormal potentials, "0" represents the absence of any noticeable spontaneous abnormal potentials, while "1" indicates the presence of various patterns of spontaneous abnormal potentials detected.

nEMG differences in CMI patients with syringomyelia involving C1 and those not involving C1

Compared to the group with syringomyelia not involving C1, the group involving C1 showed further prolongation in Average latency and polyphasic-adjusted average latency ($P > 0.05$), and an increase in average amplitude (not statistically significant, $P > 0.05$). Other parameters showed no significant differences (Table 5; Fig. 3).

Discussion

Long-neglected damage to RCPmi in CMI

The RCPmi is governed by the posterior branch of the C1 nerve root[20,21], situated just behind the CCJ. It is anchored to the dura via MDBs (Fig. 4A). RCPmi's abundance of slow-twitch fibers[22] and muscle spindles[23] provide it with strong proprioceptive capabilities and a role in anti-gravity functions. Research confirms its vital functions in enhancing CCJ-CSF circulation and stabilizing the atlanto-occipital joint[9].

Previously, CMI was mainly attributed to CCJ-CSF circulation obstruction due to cerebellar tonsil herniation[4,24,25]. Yet, with RCPmi's involvement in CSF circulation, we suggest that CMI's circulation issues stem from both tonsil herniation and RCPmi's compensatory failure, explaining why symptom severity can vary regardless of herniation size[26–28].

Moreover, whiplash injuries, leading to CMI in 23.3% of cases[29,30], typically cause RCPmi atrophy or fat infiltration[31,32]. Considering RCPmi's susceptibility to traction injuries from whiplash, could such injuries disrupt CCJ-CSF flow by damaging the C1 nerve or RCPmi, leading to a pressure differential in the craniovertebral area and thus a passive descent of the cerebellar tonsils (CMI)?

nEMG data for normal adults

Hallgren and colleagues[17,18] studied RCPmi in normal individuals using sEMG. Their results indicated that electromyographic activity of RCPmi did not change significantly under different directional forces, leading the authors to suggest that RCPmi's function might be to maintain stability of the joint surfaces in the occipitocervical region.

In our study, nEMG parameters for healthy adults showed that both average latency and amplitude of RCPmi remained relatively stable (Table 2), suggesting that RCPmi indeed plays a crucial role in maintaining the

Variable	Tonsillar herniation ≤ C1 (N1 = 15)	Tonsillar herniation > C1 (N3 = 25)	X^2/Z/t	*p* value
Sex			0.673	0.412
Female	7 (46.70)	15 (60.00)		
Male	8 (53.30)	10 (40.00)		
Age	45.20 ± 9.25	46.28 ± 11.51	−0.308	0.76
Average latency (ms) (R)	11.50 (10.10, 12.80)	11.70 (10.45, 12.95)	−0.447	0.655
Average latency (ms) (L)	11.72 ± 1.57	12.20 ± 1.79	−0.865	0.393
Average amplitude (uv) (R)	364.00 (291.0, 469.00)	379.00 (335.50, 431.5)	−0.964	0.335
Average amplitude (uv) (L)	331.00 (250.00, 468.00)	372.00 (311.00, 417.00)	−0.587	0.557
Polyphasic wave ratio % (R)	9.00 (0.00, 20.00)	7.10 (0.00, 12.40)	−0.155	0.877
Polyphasic wave ratio % (L)	7.50 (0.00, 18.80)	5.60 (0.00, 10.25)	−0.933	0.351
Polyphasic-adjusted average latency (R)	11.28 ± 1.54	11.54 ± 1.64	−0.497	0.622
Polyphasic-adjusted average latency (L)	11.32 ± 1.25	11.90 ± 1.95	−1.021	0.314
Amplitude mv (R)	1.60 (1.20, 1.90)	1.50 (1.10, 1.80)	−1.236	0.216
Amplitude mv (L)	1.58 ± 0.42	1.37 ± 0.43	1.53	0.134
Recruitment phase (R)			0.86	0.354
0	7 (46.70)	8 (32.00)		
1	8 (53.30)	17 (68.00)		
Recruitment phase (L)			1.143	0.285
0	6 (40)	6 (24)		
1	9 (60)	19 (76)		
Spontaneous abnormal potentials (R)			0.027	0.87
0	8 (53.3)	14 (56)		
1	7 (46.7)	11 (44)		
Spontaneous abnormal potentials (L)			3.259	0.071
0	11 (73.3)	11 (44)		
1	4 (26.7)	14 (56)		

Table 4. Comparison of EMG parameters between CMI patients with and without of cerebellar tonsillar herniation beyond C1. R represents the right RCPmi, and L represents the left RCPmi. Parameters with statistical differences are highlighted in bold. In the recruitment phase, "0" represents interference or mixed pattern, while "1" represents simple pattern. In spontaneous abnormal potentials, "0" represents the absence of any noticeable spontaneous abnormal potentials, while "1" indicates the presence of various patterns of spontaneous abnormal potentials detected.

balance of the occipitocervical joint. When patients performed Valsalva maneuvers (such as coughing, sneezing, laughing, or even swallowing), there were intense and dense contractions of electrical signals (Fig. 2D). This indicates that RCPmi, through instantaneous forceful adjustments of the dural tension at the CCJ, accelerates the CSF jet at the CCJ, thereby maintaining stable intracranial pressure—an essential function that is closely related to the pathophysiology of CMI (Fig. 4B).

Widespread denervation of RCPmi in CMI

Our nEMG results indicate that compared to healthy individuals, the CMI group exhibits extensive evidence of denervation in RCPmi.

First, when muscle fibers lose their nerve supply, they are reinnervated by the sprouting of new lateral branches from the surrounding normal nerves. These new nerve fibers are typically thinner and less well-myelinated, leading to slowed nerve impulse conduction, i.e., prolonged latency[33–35]. Our results show that both the average latency and the polyphasic-adjusted average latency in bilateral RCPmi of CMI patients are significantly prolonged by approximately 1.5 ms (Table 2; Fig. 3).

Furthermore, the remaining nerve fibers attempt to innervate more muscle fibers to compensate for the lost nerve fibers (motor unit remodeling)[36]. Because each motor unit innervates a larger number of muscle fibers, when these fibers contract simultaneously (during light contraction), each motor unit generates a larger electrical potential. This is consistent with our findings of increased average amplitude in CMI patients (by about 20uv) (Table 2; Fig. 3), although this difference has not yet reached statistical significance and requires further verification with a larger sample size.

However, despite the compensation by new nerve sprouts, the total number of muscle fibers involved in contraction is still reduced during intense contraction (IP), hence the ultimate reduction in recruitment phase amplitude[33,34]. This aligns with our findings of a lower recruitment phase amplitude in CMI-RCPmi compared to healthy individuals (average reduction of about 0.35 mv) (Table 2; Fig. 3).

Variable	SM position without C1 ($N_1 = 13$)	SM position with C1 ($N_2 = 27$)	X^2/Z/t	*p* value
Sex			0.333	0.564
Female	8 (61.50)	14 (51.90)		
Male	5 (38.50)	13 (48.10)		
Age	48.00 (37.00, 53.00)	48.00 (39.00, 55.00)	− 0.333	0.739
Average latency (ms) (R)	11.70 (10.10, 12.95)	11.70 (10.20, 12.60)	− 0.173	0.862
Average latency (ms) (L)	11.36 ± 1.46	12.34 ± 1.75	− 1.742	0.09
Average amplitude (uv) (R)	384.00 (299.50, 426.00)	371.00 (328.00, 469.00)	− 0.13	0.897
Average amplitude (uv) (L)	346.54 ± 94.75	397.07 ± 116.82	− 1.357	0.183
Polyphasic wave ratio % (R)	9.10 (0.00, 17.35)	7.70 (4.80, 11.80)	− 0.117	0.907
Polyphasic wave ratio % (L)	5.60 (0.0, 14.05)	6.30 (0.00, 12.50)	− 0.267	0.789
Polyphasic-adjusted average latency (R)	11.45 ± 1.95	11.44 ± 1.42	0.031	0.975
Polyphasic-adjusted average latency (L)	**10.73 ± 1.62**	**12.14 ± 1.61**	**− 2.579**	**0.014**
Amplitude mv (R)	1.50 (1.10, 1.55)	1.50 (1.20, 1.90)	− 1.089	0.276
Amplitude mv (L)	1.42 ± 0.51	1.46 ± 0.40	− 0.245	0.807
Recruitment phase (R)			1.709	0.191
0	3 (23.10)	12 (44.40)		
1	10 (76.90)	15 (55.60)		
Recruitment phase (L)			0.005	0.941
0	4 (30.8)	8 (29.6)		
1	9 (69.2)	19 (70.4)		
Spontaneous abnormal potentials (R)			0.609	0.435
0	6 (46.2)	16 (59.3)		
1	7 (53.8)	11 (40.7)		
Spontaneous abnormal potentials (L)			0.333	0.564
0	8 (61.5)	14 (51.9)		
1	5 (38.5)	13 (48.1)		

Table 5. Comparison of EMG parameters between CMI patients with and without SM position C1. R represents the right RCPmi, and L represents the left RCPmi. Parameters with statistical differences are highlighted in bold. In the recruitment phase, "0" represents interference or mixed pattern, while "1" represents simple pattern. in spontaneous abnormal potentials, "0" represents the absence of any noticeable spontaneous abnormal potentials, while "1" indicates the presence of various patterns of spontaneous abnormal potentials detected.

Additionally, as new or regenerating nerve fibers begin to reinnervate muscles, the likelihood of observing simple or mixed phases during intense muscle contraction significantly increases[33,34]. This was observed in our CMI patients, where the proportion of simple phases reached a remarkable 70% (Table 2).

Lastly, when muscles lose nerve supply, the postsynaptic membrane and endplate region become highly sensitive to neurotransmitters like acetylcholine, hence the manifestation of spontaneous abnormal potentials at rest[33]. This was significantly higher in our CMI patients (45% vs. 10% of healthy) (Table 2).

In conclusion, our study reveals significant denervation damage in bilateral RCPmi of CMI patients. Although this prospective double-blind evidence is quite reliable, it still requires further validation through multi-center large data studies.

Pathophysiological value of RCPmi denervation in CMI

When humans cough, RCPmi exhibits intense reactive electrical signals (Fig. 2D), indicating that when intracranial pressure (ICP) increases sharply, the body simultaneously stimulates RCPmi to contract intensely. Through myodural bridges (MDBs), RCPmi powerfully pulls on the CCJ dura, helping to accelerate the CCJ-CSF jet and buffer the sudden increase in ICP (Fig. 4B).

In asymptomatic CMI patients, during Valsalva maneuvers, when ICP suddenly increases, the cerebellar tonsils shift noticeably towards the CCJ, obstructing the CCJ-CSF pathway. However, if RCPmi functions well, it can also contract powerfully at the same time, temporarily expanding the arachnoid space at the CCJ to promote rapid CSF flow and alleviate this sudden pressure (Fig. 4C). After the Valsalva maneuver ends, the cerebellar tonsils may rebound appropriately, thus restoring a relatively balanced state.

In symptomatic CMI patients, after a sudden increase in ICP, the CVJ also encounters physical obstruction due to herniation of the cerebellar tonsils, compressing the C1 nerve root and causing denervation damage to RCPmi. Because of this, RCPmi contracts weakly, leading to insufficient CCJ-CSF flow, further increasing the pressure differential at the craniovertebral junction, pushing the cerebellar tonsils further downward, and exacerbating the compression on the C1 and even C2 nerve roots. The sensory fibers of the C1 nerve root then radiate this stimulation to the occipitocervical region, forming the typical Valsalva headache. Additionally,

due to the denervation damage, RCPmi's proprioceptive function is compromised, leading to craniovertebral instability and exacerbating occipitocervical headaches. Chronic headaches can also aggravate the contraction, fatigue, and even inflammatory necrosis of RCPmi (or the entire suboccipital muscle group), further impairing RCPmi's function and thus creating a vicious cycle (Figs. 4D and 5).

Causes of RCPmi denervation

Degree of tonsillar herniation

The tip of a herniated cerebellar tonsil can compress the C1 nerve (especially the posterior branch)[37,38]. In our study, we classified the degree of tonsillar herniation (TH) into groups: > C1 and ≤ C1. The RCPmi in the group exceeding C1 exhibited a more severe tendency for denervation (Table 4; Fig. 3). Previous research has also found that the more severe the TH, the more likely patients are to exhibit typical headaches, believed to be due to the compression of the C1 nerve root by the cerebellar tonsils[38,39]. However, we believe that the compression of the C1 by the cerebellar tonsils is multifactorial. Apart from the degree of herniation, it also closely relates to the compliance of the cerebellar tonsils, the degree of ventral displacement[38], the pulsation of the cerebellar tonsils[40,41], etc. Therefore, in our study, the degree of TH only partially affects the nEMG parameters of RCPmi (Table 4; Fig. 3).

Therefore, in clinical practice, patients with CMI who exhibit cerebellar tonsillar herniation extending beyond the level of the C1 vertebra may be at risk of C1 nerve root compression. However, only those patients who concurrently present with significant denervation of the RCPmi necessitate opening the dura mater for exploration and neural decompression.

While PFD unavoidably leads to damage or even complete disruption of the RCPmi—rendering intraoperative decompression of the C1 nerve root ineffective in alleviating postoperative denervation of the RCPmi—the C1 nerve root and its branches also innervate two other muscles with similar functions and associated MDBs[42,43]: the Obliquus Capitis Inferior and the Rectus Capitis Posterior Major, as well as numerous other suboccipital muscle groups. Therefore, releasing the C1 nerve root can aid in restoring the function of these muscles.

Moreover, the sensory fibers of the C1 nerve root contribute to the sensory perception of the occipitocervical region. Decompressing the compressed C1 nerve root can help alleviate the typical cervico-occipital pain symptoms. Consequently, it is necessary during surgery to perform intradural exploration and decompression of the C1 nerve root in patients whose cerebellar tonsillar herniation extends beyond C1 and who have severe denervation of the RCPmi.

High-positioned syringomyelia

Syringomyelia can cause denervation damage to the paravertebral muscles and even lead to scoliosis[44]. In our high-positioned Syringomyelia group, RCPmi indeed showed a more severe tendency for denervation (Table 4; Fig. 3). However, we also observed that many patients without Syringomyelia exhibited denervation damage to RCPmi. Thus, we believe the impact of Syringomyelia on denervation is partial. Besides, other spinal factors possibly related to RCPmi denervation damage in CMI patients may include: abnormal oscillation of the high cervical spinal cord[45–47], widespread micro-damage to the medulla oblongata[48], and direct developmental defects of the mesodermal nerves, etc[47].

Although Syringomyelia can cause certain denervation damage to RCPmi, it is more likely a result of the exacerbation of CCJ-CSF circulation disorders caused by RCPmi damage. Thus, for CMI patients, treating denervation of RCPmi might take precedence over direct treatments for Syringomyelia (such as spinal shunting).

Other potential factors: inflammation of C1 branch and cervicomedullary injury

The long-term chronic pain in the occipitocervical region of CMI patients instinctively leads the body to attempt to limit further damage and pain, thereby causing muscle tension or contraction, and releasing a large amount of inflammatory mediators[49]. These inflammatory mediators further stimulate the deep cervical nerves and cause a vicious cycle of denervation damage to RCPmi (Figs. 4 and 5). Therefore, for CMI patients with long-term chronic occipitocervical pain, appropriate pain relief and anti-inflammatory treatment are key to breaking this vicious cycle[50–52].

Long-term chronic headaches can also cause compression or even diffuse damage to the white matter of the entire brain area in CMI patients, as well as direct compression of the cervicomedullary conducting fibers by the cerebellum or tonsils[48,53–55]. This can weaken the nervous system's control over RCPmi and other suboccipital muscle groups, exacerbating denervation damage to RCPmi (Figs. 4 and 5). At this time, thorough CCJ decompression is crucial[3,4].

The relationship between RCPmi denervation and Chiari headache

Controversy over the morphological changes of RCPmi in headaches

CMI patients frequently experience occipitocervical pain, reported by up to 78%, with occipital Valsalva headaches comprising 48% of cases[2]. Research connects these symptoms to morphological changes in RCPmi.

Fernandez et al.[56] and Fernández[57] noted reduced RCPmi size in patients with chronic headaches, linking RCPmi activity to pain and atrophy. Fakhran et al.[58] observed significant headaches in patients with post-traumatic RCPmi atrophy. Min et al.[59] further associated more severe headaches with greater atrophy in chronic tension-type headache patients ($n = 15$).

However, conflicting data exists. Yuan et al.[60] found RCPmi hypertrophy in some patients, while Hvedstrup et al.[61] saw no structural differences in RCPmi between chronic migraine sufferers and controls. These inconsistencies may stem from unclear headache classifications. Additionally, the inherently small size of the RCPmi makes it susceptible to demographic influences, and the low sample sizes in some studies can easily lead

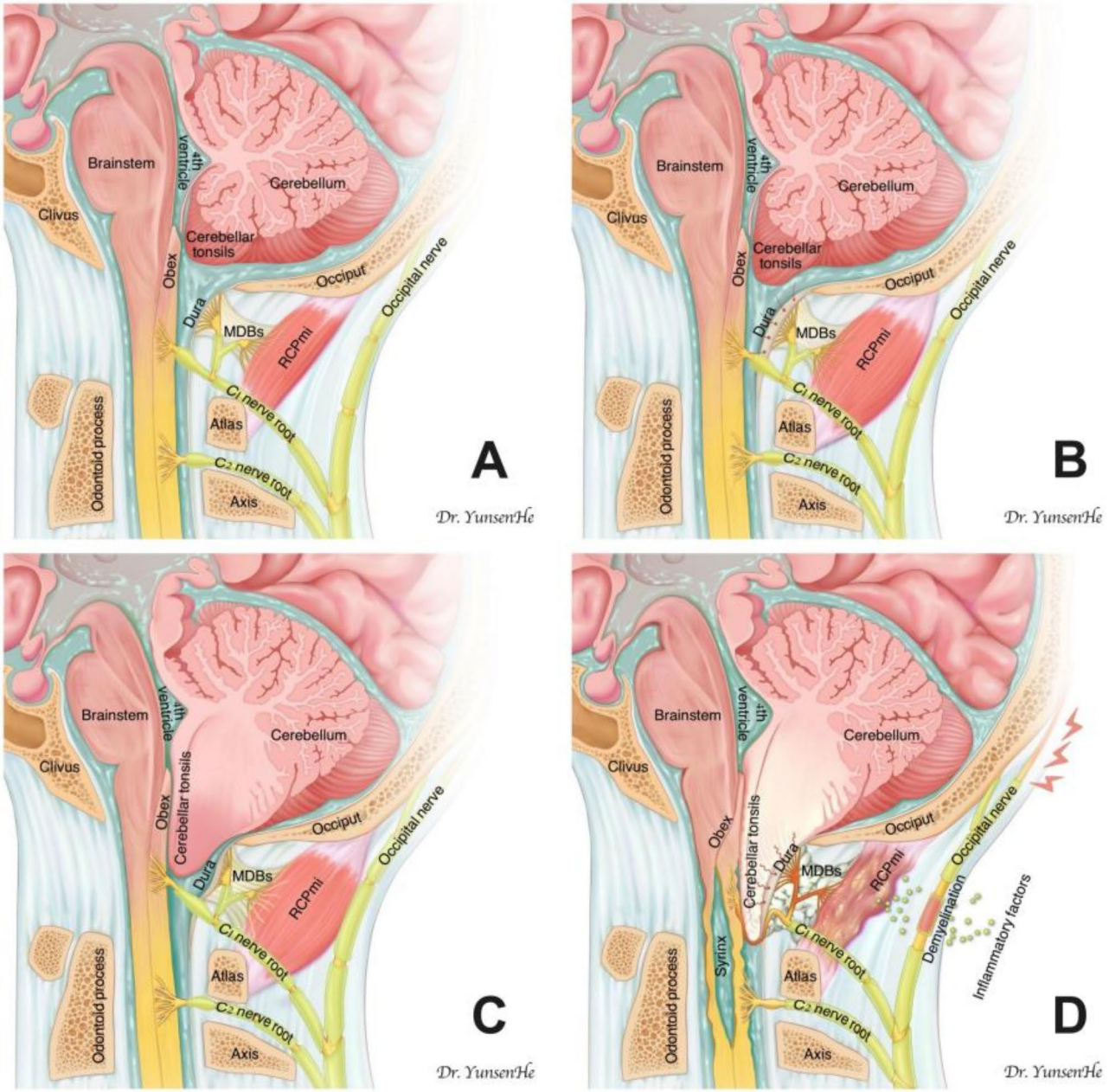

to systematic errors in measurements. Hence, functional nEMG testing of RCPmi might provide more accurate assessments than morphological studies alone.

The relationship between CMI headaches and the C1 nerve root

In our study, 62.5% (25/40) of CMI patients exhibited related headaches, and those with headaches showed more severe denervation damage to RCPmi (Table 3; Fig. 3). We believe this is due to the fact that both the motor nerves that innervate RCPmi and the sensory nerves that induce headaches in the occipital and upper cervical regions are innervated (or partially innervated) by the C1 nerve root (Fig. 4A).

First, Noseda et al.[62] showed through a rat model that high cervical nerves can reflect occipital pain in rats. As early as 2013, Johnston et al.[63] awakened 10 patients undergoing cranio-cervical surgery for headaches intraoperatively by stimulating the C1 nerve root, successfully inducing typical occipital headaches and migraines. Our previous research[2] also proved that occipital headaches (48%) and migraines (29%) coexist in CMI patients. Recently, Morgenstern et al.[38] also proposed in their study of CM 0.5 type (Tonsillar descent and presence of ventral herniation): "One of the possible causes of headache development is cervical root compression."

Additionally, recently, Almutairi et al.[50] successfully treated patients with cough-induced Valsalva occipital headaches through simple Occipital Nerve Blockade. Since cough-induced Valsalva occipital headaches are the most typical symptom in CMI patients, perhaps the typical headaches in CMI patients are also closely related to the Occipital Nerve and can be treated minimally invasively in this manner.

In conclusion, we have ample reason to believe that previous understandings of headaches in CMI patients may be incorrect. The classical theory holds that CMI headaches are closely related to CCJ-CSF fluid dynamic

◀**Fig. 4**. Mechanism of action and anatomical relationships of RCPmi in normal populations and CMI patients. (**A**) Anatomical mechanism of RCPmi at the CCJ area in resting state healthy individuals. In healthy individuals at rest or during low-intensity activities, RCPmi maintains a relatively stable, continuous light contraction state, ensuring stability of the occipitocervical joint and relaxation of the CCJ dura during daily activities. (**B**) Physiological mechanism of RCPmi at the CCJ area during Valsalva maneuvers in healthy individuals. When healthy individuals experience a sudden increase in ICP during Valsalva maneuvers or other causes, the cerebellar tonsils move rapidly towards the CCJ, and the CCJ-CSF flow speed increases sharply. RCPmi reacts by contracting, pulling on the CCJ dura through MDBs to expand outward, increasing the arachnoid space at the CCJ, helping the CCJ-CSF jet flow. (**C**) Anatomical mechanism of RCPmi at the CCJ area in asymptomatic CMI patients during Valsalva maneuvers or other causes of sudden ICP increase. In asymptomatic CMI patients during Valsalva maneuvers, ICP increases sharply, the cerebellar tonsils move noticeably towards the CCJ, and obstruct the CCJ. Meanwhile, RCPmi contracts intensely, pulling on MDBs, causing significant dorsal expansion of the CCJ dura, instantly expanding the arachnoid space at the CCJ to promote rapid CSF flow through the CCJ, quickly alleviating this sudden ICP pressure. After the Valsalva maneuver ends, the cerebellar tonsils appropriately rebound, thus restoring a relatively balanced state at the CCJ. (**D**) Pathological mechanism of RCPmi at the CCJ area in symptomatic CMI patients during Valsalva maneuvers. In symptomatic CMI patients during Valsalva maneuvers or other causes of sudden ICP increase, the CCJ also encounters physical obstruction from herniation of the cerebellar tonsils, also compressing the posterior branch of the C1 nerve root and causing denervation damage to RCPmi (fat liquefaction, atrophy, inflammation, sclerosis). Because of this denervation, RCPmi contracts weakly, leading to insufficient CCJ-CSF flow, further increasing the pressure differential at the CCJ, pushing the cerebellar tonsils further downward, and exacerbating the compression on the CRN1/2. The sensory fibers of the CRN1 then radiate this stimulation to the occipitocervical region, forming the typical Valsalva headache. Meanwhile, the cerebellar tonsils undergo chronic herniation compression, gradually becoming ischemic pale, sclerotic, and losing elasticity. MDBs, under long-term overload and inflammatory infiltration, gradually become sclerotic and lose compliance. While the CCJ-Dura, under long-term traction by MDBs, compression friction by the cerebellar tonsils, and inflammatory factor infiltration, gradually thickens and loses compliance. Due to completely obstructed CCJ-CSF flow, syringomyelia gradually forms. Because of compression by the cerebellar tonsils, syringomyelia, inflammatory factor infiltration, and cervicomedullary injury, the CRN1 suffers damage and demyelination reactions, participating in and exacerbating the vicious cycle of RCPmi denervation damage, occipitocervical headaches, etc. *C1* cervical vertebra 1, *ICP* intracranial pressure, *CVJ* craniovertebral junction, *CSF* cerebrospinal fluid, *RCPmi* rectus capitis posterior minor, *MDBs* muscle-dural bridges, *CRN1* C1 nerve root.

disturbances[64–71]. We believe that headaches in CMI patients are mainly related to compression or stimulation of the C1 nerve root and its branches (Figs. 4 and 5).

The relationship between CMI headaches and RCPmi denervation

Firstly, compression of the C1 nerve root simultaneously causes occipitocervical headaches and denervation damage to RCPmi. And the damage to RCPmi then triggers instability in the occipitocervical area, leading to long-term chronic headaches.

Simultaneously, in symptomatic CMI patients, a herniated cerebellum or cerebellar tonsils also stimulate the CCJ dural receptors (also innervated by branches of the posterior branch of the C1 nerve root[20,21]). On one hand, CCJ dural receptors can radiate these stimuli to the occipitocervical region to form pain; on the other hand, CCJ dural receptors can also induce more intense contractions of RCPmi, attempting to pull on the CCJ dura more forcefully, producing more CCJ-CSF flow. And this can lead to continuous overload, stiffness, inflammation, and fat infiltration of RCPmi. The C1 nerve, greater occipital, lesser occipital nerves, and their branches passing through these diseased muscle groups might be compressed or stimulated by inflammation, further forming occipitocervical pain (Figs. 4D and 5).

Our results show that occipitocervical pain in CMI patients is closely related to degenerative damage to the suboccipital muscle group. Therefore, treating pain and relaxing the suboccipital muscle group while simultaneously alleviating the compression or damage to the C1 nerve is a new target for treating CMI patients.

Clinical applications of RCPmi denervation in the treatment of CMI

In recent years, numerous reports have emerged on the non-surgical treatment of patients with Chiari malformation type I (CMI)[50,72–79]. Some physiotherapy programs have inadvertently produced therapeutic effects on the RCPmi, leading to clinical improvements. This year, we administered targeted rehabilitation therapy focusing on the RCPmi to four CMI patients with significant symptoms who declined surgical intervention. All patients experienced varying degrees of symptom relief. Interestingly, post-treatment electrophysiological reassessment of their RCPmi revealed partial recovery from denervation in two patients. Although the follow-up period is currently short and the sample size is limited, these findings suggest that rehabilitation therapy targeting the RCPmi may be effective for some CMI patients.

Furthermore, for patients requiring surgical intervention, it is crucial to protect the RCPmi and other suboccipital muscle groups. Clinically, there are numerous cases where patients develop CSF flow disturbances at the CCJ and hydrocephalus following PFD surgery for CMI—occurring in approximately 7% of cases. This includes patients who have undergone only bony decompression[80–87]. In 2023, we encountered two such CMI patients and believe that excessive intraoperative damage to the RCPmi and suboccipital muscles was related

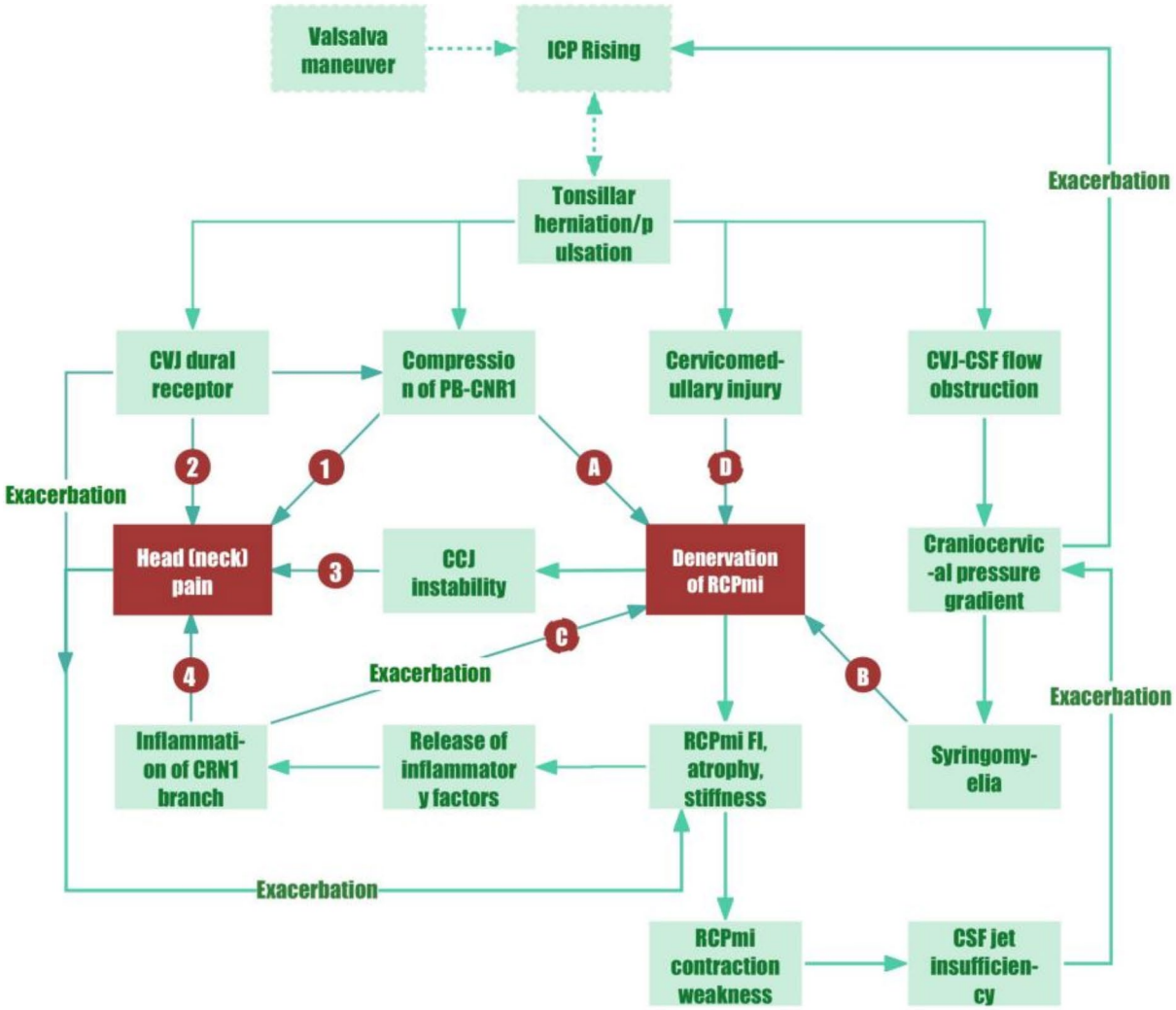

Fig. 5. System Mapping flowchart of the pathological processes related to the CCJ in CMI patients during Valsalva maneuvers or daily cerebellar tonsils pulsate. As shown in the diagram, there are three factors causing Denervation of RCPmi: (**A**) Compression of PB-CNR1 by tonsillar; (**B**) Syringomyelia; (**C**) Inflammation of CNR1 branch; (**D**) Cervicomedullary injury. And there are four mechanisms causing Head (neck) pain: ① Compression of CNR1 by tonsillar herniation/pulsation; ② Stimulation of CCJ dural receptors by tonsillar; ③ CCJ instability; ④ Inflammation of C1 branch. *ICP* intracranial pressure, *CCJ* craniocervical junction, *CNR1*. *C1* nerve root, *PB-CNR1* posterior branch of the CNR1, *CSF* cerebrospinal fluid, *RCPmi* rectus capitis posterior minor, *FI* fat infiltration.

to their postoperative complications. Consequently, minimally invasive decompression techniques using small portals have been proposed in recent years to minimize damage to the suboccipital muscles and myodural bridges, yielding favorable outcomes[88–91].

Finally, regarding traditional PFD surgeries, it is essential not only to minimize disruption from the surgical approach but also to strictly control the indications for opening the dura mater to avoid the complications. For patients with severe RCPmi denervation and typical headaches, it is important to assess whether the C1 nerve root is compressed. Additionally, since the surgery disrupts the RCPmi—eliminating its traction effect on the CVJ dura mater[9]—excessive dural repair should be avoided during surgery. This precaution helps prevent folding and collapse of the dura mater during postoperative movements, which could adversely affect CSF flow at the CVJ. Moreover, the RCPmi's role in monitoring atlanto-occipital joint stability[9] is also compromised due to surgical damage. Therefore, intraoperative excessive bone removal should be minimized to prevent postoperative instability of the atlanto-occipital joint.

Limitations and prospects

1. Small sample size, which led to most observed differences within CMI subgroups lacking statistical significance, and no asymptomatic CMI patients were collected to verify some of our theories.
2. Demographic bias of a single-center study
3. In addition to RCPmi, muscles that can affect CCJ-CSF flow or stability of the CCJ include RCPma, suboccipital oblique muscles, etc[42]. However, due to the safety and variable control of nEMG testing, we only studied RCPmi. But the real situation might be that the entire suboccipital muscle group and muscle-dural bridge group are working together, which requires further research to explore this complex mechanism.
4. The C1 nerve root has many motor fibers but few sensory fibers, so it may only play a partial role in occipitocervical pain. The C2 nerve root might also play an important role, and it is also easily damaged in CMI. For the sake of safety and simplicity of analysis in nEMG, C2 was not included in this study, which requires further research in the future.

Conclusion

1. The nEMG parameters of RCPmi in healthy adults remain relatively constant at rest or during light contraction, indicating its role in maintaining the stability of the occipitocervical joint. Additionally, during normal daily Valsalva maneuvers, RCPmi plays an important role in maintaining constant ICP.
2. Compared to the healthy control group: CMI patients exhibit widespread denervation damage in RCPmi. This may cause further exacerbation and symptom manifestation of CCJ-CSF fluid dynamic disturbances in CMI patients. However, the causal relationship between the two requires further research.
3. The cause of RCPmi denervation damage may stem from compression of the C1 nerve root by the herniated cerebellar tonsil, stimulation of CCJ dural receptors (from compression of posterior cranial fossa brain tissue or excessive pulling of RCPmi), overload of RCPmi and other deep cervical muscles, high-positioned syringomyelia, and other pathological factors.
4. Occipitocervical headaches in CMI patients are mainly related to stimulation of sensory fibers of the C1 nerve root, often occurring simultaneously with RCPmi denervation damage, which may be a new target for treating CMI.
5. nEMG of high cervical deep muscles is safe and reliable, and can be widely used in diseases such as CMI, chronic occipitocervical pain, cervical spondylosis, and whiplash injury.

Data availability

The datasets used and/or analysed during the current study available from the corresponding author on reasonable request.

Received: 5 July 2024; Accepted: 13 January 2025
Published online: 17 March 2025

References

1. He, Y. et al. Research process, recap, and prediction of Chiari malformation based on bicentennial history of nomenclature and terms misuse. *Neurosurg. Rev.* **46**(1), 316 (2023).
2. He, Y. et al. Prevalence and treatment of typical and atypical headaches in patients with Chiari I malformation: A meta-analysis and literature review. *Cephalalgia* **43**(1), 3331024221131356 (2023).
3. He, Y. et al. Significance of modified clivoaxial angles in the treatment of adult chiari malformation type I. *World Neurosurg.* **130**, e1004–e1014 (2019).
4. He, Y. et al. A novel craniocervical junction compression severity index-based grading system for multidirectional quantification of the biomechanics at foramen magnum of Chiari malformation type I. *J. Neurolog. Surg. Part B Skull Base* **84**, 616–628 (2022).
5. McClugage, S. G. & Oakes, W. J. The Chiari I malformation. *J. Neurosurg. Pediatr.* **24**(3), 217–226 (2019).
6. Taylor, D. G. et al. Two distinct populations of Chiari I malformation based on presence or absence of posterior fossa crowdedness on magnetic resonance imaging. *J. Neurosurg.* **126**(6), 1934–1940 (2017).
7. Bao, M. et al. Large vestibular schwannoma presenting in late state of pregnancy—A case report and literature review. *Front. Neurol.* **14**, 1270989 (2023).
8. He, Y. et al. Unveiling the domino effect: A nine-year follow-up on pentalogy of central nervous system induced by a large unruptured cerebral arteriovenous malformation: A case report and literature review. *Front. Neurol.* **15**, 1365525 (2024).
9. Zheng, N. et al. The universal existence of myodural bridge in mammals: An indication of a necessary function. *Sci. Rep.* **7**(1), 1–9 (2017).
10. Li, C. et al. The relationship between myodural bridges, hyperplasia of the suboccipital musculature, and intracranial pressure. *PLoS ONE* **17**(9), e0273193 (2022).
11. Goel, A. Goel's classification of atlantoaxial "facetal" dislocation. *J. Craniovertebr. Junction Spine* **5**(1), 3–8 (2014).
12. Goel, A. Is atlantoaxial instability the cause of Chiari malformation? Outcome analysis of 65 patients treated by atlantoaxial fixation. *J. Neurosurg. Spine* **22**(2), 116–127 (2015).
13. Wan, M. et al. A morphometric study of the atlanto-occipital joint in adult patients with Chiari malformation type I. *Br. J. Neurosurg.* **38**, 1–4 (2020).
14. Wan, M. et al. Feasibility of occipital condyle screw placement in patients with Chiari malformation type I: A computed tomography-based morphometric study. *Acta Neurochir. (Wien)* **163**(6), 1569–1575 (2021).
15. Labuda, R. et al. A new hypothesis for the pathophysiology of symptomatic adult Chiari malformation type I. *Med. Hypotheses* **158**, 110740 (2022).
16. Hallgren, R. C. et al. A standardized protocol for needle placement in suboccipital muscles. *Clin. Anat.* **21**(6), 501–508 (2008).
17. Hallgren, R. C. & Rowan, J. J. Implied evidence of the functional role of the rectus capitis posterior muscles. *J. Am. Osteopath. Assoc.* **120**(6), 395–403 (2020).
18. Hallgren, R. C. et al. Electromyographic activity of rectus capitis posterior minor muscles associated with voluntary retraction of the head. *Spine J.* **14**(1), 104–112 (2014).

19. Gertken, J. T. et al. Risk of hematoma following needle electromyography of the paraspinal muscles. *Muscle Nerve* **44**(3), 439–440 (2011).
20. Saladin, K. S. *Human Anatomy* (Rex Bookstore, Inc, 2005).
21. Michael-Titus, A. T. & Shortland, P. *The Nervous System: The Nervous System, E-Book* (Elsevier Health Sciences, 2022).
22. Yamauchi, M. et al. Morphological classification and comparison of suboccipital muscle fiber characteristics. *Anat. Cell Biol.* **50**(4), 247–254 (2017).
23. Diao, X. et al. Research progress of chronic cervicogenic headache based on the concept of muscular dural bridge complex. *Aging Commun.* **3**(4), 16. https://doi.org/10.53388/aging2021016 (2021).
24. Buell, T. J., Heiss, J. D. & Oldfield, E. H. Pathogenesis and cerebrospinal fluid hydrodynamics of the Chiari I malformation. *Neurosurg. Clin. N. Am.* **26**(4), 495–499 (2015).
25. Shaffer, N., Martin, B. & Loth, F. Cerebrospinal fluid hydrodynamics in type I Chiari malformation. *Neurol. Res.* **33**(3), 247–260 (2011).
26. Tetik, B. et al. *Multi-parameter-based Radiological Diagnosis of Chiari Malformation Using Machine Learning Technology* (Authorea, 2021).
27. Shuman, W. H. et al. Is there a morphometric cause of Chiari malformation type I? Analysis of existing literature. *Neurosurg. Rev.* **45**, 263–273 (2021).
28. Heffez, D. S. et al. Is there a relationship between the extent of tonsillar ectopia and the severity of the clinical Chiari syndrome?. *Acta Neurochir. (Wien)* **162**(7), 1531–1538 (2020).
29. Freeman, M. D. et al. A case-control study of cerebellar tonsillar ectopia (Chiari) and head/neck trauma (whiplash). *Brain Inj.* **24**(7–8), 988–994 (2010).
30. Wan, M. J., Nomura, H. & Tator, C. H. Conversion to symptomatic Chiari I malformation after minor head or neck trauma. *Neurosurgery* **63**(4), 748–753 (2008).
31. McPartland, J. M. & Brodeur, R. R. Rectus capitis posterior minor: A small but important suboccipital muscle. *Jo. Bodyw. Mov. Ther.* **3**(1), 30–35 (1999).
32. Elliott, J. et al. Fatty infiltration in the cervical extensor muscles in persistent whiplash-associated disorders: A magnetic resonance imaging analysis. *Spine* **31**, E847–E855 (2006).
33. Rubin, D. I. Needle electromyography waveforms during needle electromyography. *Neurol. Clin.* **39**(4), 919–938 (2021).
34. Rubin, D. I. Needle electromyography: Basic concepts. *Handb. Clin. Neurol.* **160**, 243–256 (2019).
35. Preston, D. C. & Shapiro, B. E. *Electromyography and Neuromuscular Disorders E-book: Clinical-Electrophysiologic-Ultrasound Correlations* (Elsevier Health Sciences, 2020).
36. Krarup, C. et al. Remodeling of motor units after nerve regeneration studied by quantitative electromyography. *Clin. Neurophysiol.* **127**(2), 1675–1682 (2016).
37. Shao, B. et al. Reappraisal of intradural findings in Chiari malformation type I. *Neurosurg. Focus* **54**(3), E2 (2023).
38. Morgenstern, P. F. et al. Ventrolateral tonsillar position defines novel Chiari 0.5 classification. *World Neurosurg.* **136**, 444–453 (2020).
39. Huang, C. W. C. et al. Clinical utility of 2-D anatomic measurements in predicting cough-associated headache in Chiari I malformation. *Neuroradiology* **62**, 593–599 (2020).
40. Collins, R. A. et al. Association of cerebellar tonsil dynamic motion and outcomes in pediatric Chiari I malformation. *World Neurosurg.* **168**, e518–e529 (2022).
41. Tietze, M. et al. Dynamic cerebellar herniation in Chiari patients during the cardiac cycle evaluated by dynamic magnetic resonance imaging. *Neuroradiology* **61**(7), 825–832 (2019).
42. Scali, F. et al. Histological analysis of the rectus capitis posterior major's myodural bridge. *Spine J.* **13**(5), 558–563 (2013).
43. Hack, G. D., Koritzer, R. T., Robinson, W. L., Hallgren, R. C. & Greenman, P. E. Anatomic relation between the rectus capitis posterior minor muscle and the dura mater. *Spine* **20**(23), 2484–2486 (1995).
44. Zhu, Z. et al. Abnormal spreading and subunit expression of junctional acetylcholine receptors of paraspinal muscles in scoliosis associated with syringomyelia. *Spine* **32**(22), 2449–2454 (2007).
45. Klinge, P. M. et al. Abnormal spinal cord motion at the craniocervical junction in hypermobile Ehlers-Danlos patients. *J. Neurosurg. Spine* **35**, 1–7 (2021).
46. Shao, B. et al. Compromised cranio-spinal suspension in Chiari malformation type 1: A potential role as secondary pathophysiology. *J. Clin. Med.* **11**(24), 7437 (2022).
47. Thakar, S. et al. Does the mesodermal derangement in Chiari type I malformation extend to the cervical spine? Evidence from an analytical morphometric study on cervical paraspinal muscles. *J. Neurosurg. Spine* **27**(4), 421–427 (2017).
48. Houston, J. R. et al. Evidence of neural microstructure abnormalities in type I Chiari malformation: Associations among fiber tract integrity, pain, and cognitive dysfunction. *Pain Med.* **21**(10), 2323–2335 (2020).
49. Fernández-Carnero, J. et al. Neural tension technique improves immediate conditioned pain modulation in patients with chronic neck pain: A randomized clinical trial. *Pain Med.* **20**(6), 1227–1235 (2019).
50. Almutairi, A. & Chan, T. L. H. Cough headache responsive to occipital nerve blockade. *Can. J. Neurol. Sci.* **52**, 1–2 (2024).
51. Barpujari, A. et al. A systematic review of non-opioid pain management in Chiari malformation (type 1) patients: Current evidence and novel therapeutic opportunities. *J. Clin. Med.* **12**(9), 3064 (2023).
52. Fitzgerald, S. Decompression doesn't necessarily provide headache relief for patients with Chiari I malformation. *Neurol. Today* **22**(18), 8–9 (2022).
53. Antkowiak, L. et al. Clinical application of diffusion tensor imaging in Chiari malformation type I—Advances and perspectives. A systematic review. *World Neurosurg.* **152**, 124–136 (2021).
54. Gok, H. & Naderi, S. Prognostic value of craniovertebral junction diffusion tensor imaging in patients with Chiari type 1 malformation. *Turk. Neurosurg.* **30**(3), 400–406 (2020).
55. Krishna, V. et al. Diffusion tensor imaging assessment of microstructural brainstem integrity in Chiari malformation type I. *J. Neurosurg.* **125**(5), 1112–1119 (2016).
56. Fernandez-de-Las-Penas, C. et al. Magnetic resonance imaging study of the morphometry of cervical extensor muscles in chronic tension-type headache. *Cephalalgia* **27**(4), 355–362 (2007).
57. Fernández-de-Las-Peñas, C. et al. Association of cross-sectional area of the rectus capitis posterior minor muscle with active trigger points in chronic tension-type headache: A pilot study. *Am. J. Phys. Med. Rehabil.* **87**(3), 197–203 (2008).
58. Fakhran, S., Qu, C. & Alhilali, L. M. Effect of the suboccipital musculature on symptom severity and recovery after mild traumatic brain injury. *AJNR Am. J. Neuroradiol.* **37**(8), 1556–1560 (2016).
59. Min, X. et al. Relationship between changes in cranio-cervical extensor muscles and quality of life: A single-center study of 15 patients with chronic tension-type headache. *Med. Sci. Monit.* **29**, e938574 (2023).
60. Yuan, X. Y. et al. Correlation between chronic headaches and the rectus capitis posterior minor muscle: A comparative analysis of cross-sectional trail. *Cephalalgia* **37**(11), 1051–1056 (2017).
61. Hvedstrup, J. et al. Volume of the rectus capitis posterior minor muscle in migraine patients: A cross-sectional structural MRI study. *J. Headache Pain* **21**(1), 57 (2020).
62. Noseda, R. et al. Non-trigeminal nociceptive innervation of the posterior dura: Implications to occipital headache. *J. Neurosci.* **39**(10), 1867–1880 (2019).

63. Johnston, M. M., Jordan, S. E. & Charles, A. C. Pain referral patterns of the C1 to C3 nerves: Implications for headache disorders. *Ann. Neurol.* **74**(1), 145–148 (2013).
64. Bhadelia, R. A. et al. Cough-associated headache in patients with Chiari I malformation: CSF flow analysis by means of cine phase-contrast MR imaging. *AJNR Am. J. Neuroradiol.* **32**(4), 739–742 (2011).
65. Sansur, C. A. et al. Pathophysiology of headache associated with cough in patients with Chiari I malformation. *J. Neurosurg.* **98**(3), 453–458 (2003).
66. Bezuidenhout, A. F. et al. Relationship between cough-associated changes in CSF flow and disease severity in Chiari I malformation: An exploratory study using real-time MRI. *AJNR Am. J. Neuroradiol.* **39**(7), 1267–1272 (2018).
67. McGirt, M. J. et al. Correlation of cerebrospinal fluid flow dynamics and headache in Chiari I malformation. *Neurosurgery* **56**(4), 716–721 (2005) (**discussion 716–21**).
68. van Dellen, J. R. Chiari malformation: An unhelpful eponym. *World Neurosurg.* **156**, 1–3 (2021).
69. Mugge, L. et al. Headache and other symptoms in Chiari Malformation type I is associated with CSF flow improvement after decompression: a two-institutional. *World Neurosurg.* **163**, e253–e262 (2022).
70. Gholampour, S. & Gholampour, H. Correlation of a new hydrodynamic index with other effective indexes in Chiari I malformation patients with different associations. *Sci. Rep.* **10**(1), 15907 (2020).
71. Alperin, N. et al. Imaging-based features of headaches in Chiari malformation type I. *Neurosurgery* **77**(1), 96–103 (2015) (**discussion 103**).
72. Abdallah, A. et al. The factors affecting the outcomes of conservative and surgical treatment of Chiari I adult patients: A comparative retrospective study. *Neurol. Res.* **44**(2), 165–176 (2022).
73. Abdallah, A. & Rakip, U. Conservative treatment of Chiari malformation type I based on the phase-contrast MRI: A retrospective study. *World Neurosurg.* **163**, e323–e334 (2022).
74. Giallongo, A. et al. Clinicoradiographic data and management of children with Chiari malformation type 1 and 1.5: An Italian case series. *Acta Neurol. Belg.* **121**, 1547–1554 (2020).
75. Leon, T. J. et al. Patients with "benign" Chiari I malformations require surgical decompression at a low rate. *J. Neurosurg. Pediatr.* **23**(4), 498–506 (2019).
76. Lu, S. M. et al. Inferiorly directed posterior cranial vault distraction for treatment of Chiari malformations. *J. Craniofac. Surg.* **34**(1), 284–287 (2023).
77. Marianayagam, N. J. et al. Conservative management for pediatric patients with chiari 1 anomaly: A retrospective study. *Clin. Neurol. Neurosurg.* **189**, 105615 (2020).
78. Szuflita, N. S. et al. Nonoperative management of enlarging syringomyelia in clinically stable patients after decompression of Chiari malformation type I. *J. Neurosurg. Pediatr.* **28**, 1–6 (2021).
79. Türkmen, C. et al. Effects of two exercise regimes on patients with Chiari malformation type 1: A randomized controlled trial. *Cerebellum* **22**, 1–11 (2022).
80. Bartoli, A. et al. Treatment options for hydrocephalus following foramen magnum decompression for Chiari I malformation: A multicenter study. *Neurosurgery* **86**(4), 500–508 (2020).
81. De Vlieger, J., Dejaegher, J. & Van Calenbergh, F. Posterior fossa decompression for Chiari malformation type I: Clinical and radiological presentation, outcome and complications in a retrospective series of 105 procedures. *Acta Neurol. Belg.* **119**(2), 245–252 (2019).
82. Marshman, L. A. et al. Acute obstructive hydrocephalus associated with infratentorial subdural hygromas complicating Chiari malformation type I decompression: Report of two cases and literature review. *J. Neurosurg.* **103**(4), 752–755 (2005).
83. Pepper, J., Rodrigues, D. & Gallo, P. Endoscopic third ventriculostomy for hydrocephalus after craniovertebral decompression for Chiari malformation type I: Technical nuances and surgical pitfalls. *Childs Nerv. Syst.* **39**(12), 3501–3507 (2023).
84. Perrini, P. et al. Acute external hydrocephalus complicating craniocervical decompression for syringomyelia-Chiari I complex: Case report and review of the literature. *Neurosurg. Rev.* **31**(3), 331–335 (2008).
85. Prasad, G. L. & Menon, G. R. Coexistent supratentorial and infratentorial subdural hygromas with hydrocephalus after Chiari decompression surgery: Review of literature. *World Neurosurg.* **93**, 208–214 (2016).
86. Rossini, Z. et al. Subdural fluid collection and hydrocephalus after foramen magnum decompression for Chiari malformation type I: Management algorithm of a rare complication. *World Neurosurg.* **106**, e9–e15 (2017).
87. Zakaria, R. et al. Raised intracranial pressure and hydrocephalus following hindbrain decompression for Chiari I malformation: A case series and review of the literature. *Br. J. Neurosurg.* **26**(4), 476–481 (2012).
88. Fan, T. Letter to the Editor. Critical points for consideration on minimally invasive surgery decompression alternatives for craniocervical junction-related syringomyelia. *J. Neurosurg. Spine* **34**, 1–2 (2020).
89. Mandel, M. et al. Minimally invasive foramen magnum durectomy and obexostomy for treatment of craniocervical junction-related syringomyelia in adults: Case series and midterm follow-up. *J. Neurosurg. Spine* **33**, 1–10 (2020).
90. Quillo-Olvera, J. et al. Minimally invasive craniocervical decompression for Chiari 1 malformation: An operative technique. *J. Neurol. Surg. A Cent. Eur. Neurosurg.* **80**(4), 312–317 (2019).
91. Zagzoog, N. & Reddy, K. K. Use of minimally invasive tubular retractors for foramen magnum decompression of Chiari malformation: A technical note and case series. *World Neurosurg.* **128**, 248–253 (2019).

Acknowledgement

We thank Chief physician Ying Liu and Meiyun Hu (Sichuan Provincial People's Hospital Electrophysiological center) for their guidance in electrophysiology.

Author contributions

Yunsen He, Qinjiang Huang, and Minbing Bao contributed equally to this work and should be regarded as joint first authors. All authors made substantial contributions to the study design, date collection, methodology, software, original draft, critical revision, and final approval of this manuscript.Bo Wu and Zhou Zhang contributed equally to the conception, drafting, and revision of the manuscript, and provided financial and equipment support. They should be recognized as co-corresponding authors.

Funding

Funding was provided by Natural Science Foundation of Sichuan Province (Grant No. 2023YFS0272). Health Commission of Chengdu City, Jinniu District (Grant No. JNKY2024-103) Sichuan Medical and Health Care Promotion Institute (Grant No. KY2023SJ0231).

Declarations

Competing interests
The authors declare no competing interests.

Additional information
Correspondence and requests for materials should be addressed to Z.Z. or B.W.

Reprints and permissions information is available at www.nature.com/reprints.

Publisher's note Springer Nature remains neutral with regard to jurisdictional claims in published maps and institutional affiliations.